Comparing the Validity of Statistical and Knowledge-Based Methods for Landslide Susceptibility Mapping

J. Mosaffaie[1*], A. Salehpour Jam[1], and M. R. Tabatabaei[1]

ABSTRACT

In the Shahroud Watershed, there has been an increasing occurrence of landslides that have caused a lot of human and financial losses. Therefore, landslide susceptibility zonation is crucial for reducing landslide risk. The aim of this study was to compare the Landslide Susceptibility Maps (LSMs) of different methods. Therefore, thematic layers of the ten causal factors were prepared. Then, a landslide inventory map consisting of 104 landslides covering 1401 hectares was compiled and partitioned into two subsets including 70% for training and 30% for testing purposes. Three landslide susceptibility maps were prepared using the Frequency ratio (Fr), Statistical index (Si), and Analytic Hierarchy Process (AHP) methods. The validation process showed that the Si [Area Under the Curve (AUC)= 0.732] and Fr (AUC= 0.707) models presented a more valid LSM than AHP (AUC= 0.651) method. The Qs (Quality sum) index values also confirmed the results of the ROC (Receiver Operating Characteristic) curve such that the Qs index values of 1.71, 1.43, and 0.62 for, respectively, Fr, Si, and AHP models implied a more accurate LSMs of the Fr and Si models than the one from the AHP. The results of this study can be used as a basic step for landslide risk management in the study area.

Keywords: Analytic Hierarchy Process, Bivariate statistic, Landslide hazard, Shahroud, Zonation.

INTRODUCTION

Landslides are among the most damaging natural disasters that commonly cause many socio-economic problems, especially in mountainous regions (Armin *et al*., 2019; Mosaffaie and Salehpour Jam, 2021). They have significant adverse impacts on people's lives, property, farmlands, infrastructures, and natural environments (Joybari *et al*., 2017; Mosaffaie and Salehpour Jam, 2018). According to the Iranian landslide working party, 187 people were killed and losses were estimated at 12,700 dollars until the end of September 2007(Gholami *et al*., 2019; Mosaffaie *et al*., 2015).

Causal analysis and zoning of natural hazards are essential for managing environmental issues *(Karimi Sangchini et*

al., 2022; Soltani *et al*., 2023). In this regard, identification of susceptible areas is crucial for reducing landslide-associated damages (Salehpour Jam *et al*., 2023). Landslide susceptibility zonation can help managers and decision-makers to reduce landslide risk through land use change or by preventing construction in landslide-prone areas (Karimi Sangchini *et al*., 2022; Morady *et al*., 2010; Mosaffaie *et al*., 2023; Salehpour Jam and Mosaffaie, *et al*., 2021a, 2021b; Salehpour Jam *et al*., 2023; Sangchini *et al*., 2016). Landslide susceptibility assessment methods can be classified into two main categories: (1) Statistical methods and (2) Assessments based on expert knowledge (Pradhan *et al*., 2010). Statistical methods establish a correlation between the landslide formation and affecting factors and use statistical

---

[1] Soil Conservation and Watershed Management Research Institute (SCWMRI), Agricultural Research, Education and Extension Organization (AREEO), Tehran, Islamic Republic of Iran.
* Corresponding author; e-mail: jamalmosaffaie@gmail.com

analysis to assess landslide susceptibility classifications quantitatively (Dou *et al*., 2015; Pourghasemi *et al*., 2012). Among the most common statistical models are frequency ratio (Yalcin *et al*., 2011), Artificial Neural Network (ANN) (Dou *et al*., 2015; Pradhan *et al*., 2010), decision tree approach (Saygin *et al*., 2023), logistic regression (Pourghasemi *et al*., 2013; Pradhan and Youssef, 2010), statistical index (Si) (Gholami *et al*., 2019; Ozdemir and Altural, 2013; Santos, 2015), fuzzy gamma operators (Gholami *et al*., 2019; Kanungo *et al*., 2006; Lee, 2007; Mosaffaie *et al*., 2020; Pourghasemi *et al*., 2012; Pradhan *et al*., 2009). The second category, which is subjective to some extent, requires a rating system based on experts' knowledge and experience to assess LS qualitatively. Some examples for these experts' knowledge-based methods are Analytic Hierarchy Process (AHP) (Abay *et al*., 2019; El Jazouli *et al*., 2019; He *et al*., 2019; Nguyen and Liu, 2019; Pourghasemi *et al*., 2012; Ruff and Czurda, 2008; Salehpour Jam, *et al*., 2021; Yalcin *et al*., 2011), weighted linear combination (Chen *et al*., 2017), data mining techniques (Chen *et al*., 2018; Oh and Lee, 2017), and empirical models (Armin *et al*., 2019).

Despite the existence of numerous models for landslide susceptibility assessment, there is no universally accepted model and it is important to choose an appropriate model for landslide susceptibility evaluation. In this regard, although different methods have been compared in many studies, little research has been conducted to compare knowledge-based methods with other statistical methods. Therefore, it can be hypothesized that these two groups of methods do not have the same validity.

The main aim of this study was to compare the performance of AHP as a knowledge-based method with two widely accepted statistical models including frequency ratio and statistical index at Shahroud Watershed as a hotspot area in landslide occurrence. The landslide susceptibility map resulting from the more

valid model will be very useful for better management of the watershed.

MATERIALS AND METHODS

Description of the Study Area

Shahroud Watershed is one of the main tributaries of the Sefidrood River that covers the northern part of Qazvin Province in Iran (Figure 1). This mountainous watershed with an area of 1947 km^2 covers about 22% of Qazvin Province. The average annual rainfall of the watershed is 392 mm, and mostly occurs between January to May. The watershed landscape is dominantly covered by rangelands and other land uses of the watershed are residential, dry farming, irrigated farming, orchards, forest, and bare lands (Mosaffaie, 2016). The existence of landslide predisposing factors such as mountainous topography, seismicity, and high relative seismic seismicity, landslide-sensitive geological formations, semi-humid climate, road construction, and conversion of rangelands to orchards have caused numerous destructive landslides in this watershed. Therefore, preparing landslide susceptibility map with a suitable model is necessary for better watershed management.

This study involved four main steps: Preparing the landslide causal factors, mapping the spatial distribution of landslides, landslide susceptibility analyses using selected methods, and, finally, evaluating the validity of the used methods. The ArcGIS 10 software was used for preparing different digital layers and crossing them. Conceptualization of the study has been illustrated in Figure 2.

Landslide Inventory Map

The Landslide Inventory Map (LIM) shows the characteristics of the landslides that have occurred in the past (Yalcin *et al*., 2011). In this study, the LIM was prepared using two characteristics of landslides
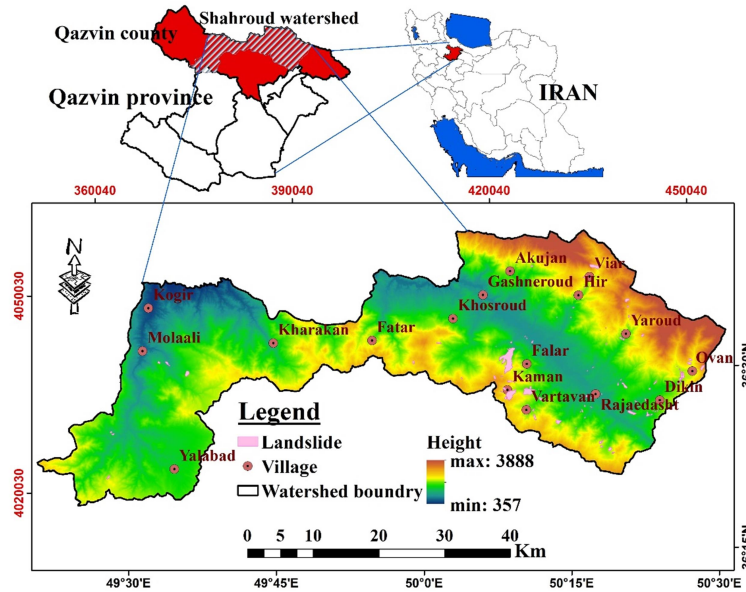
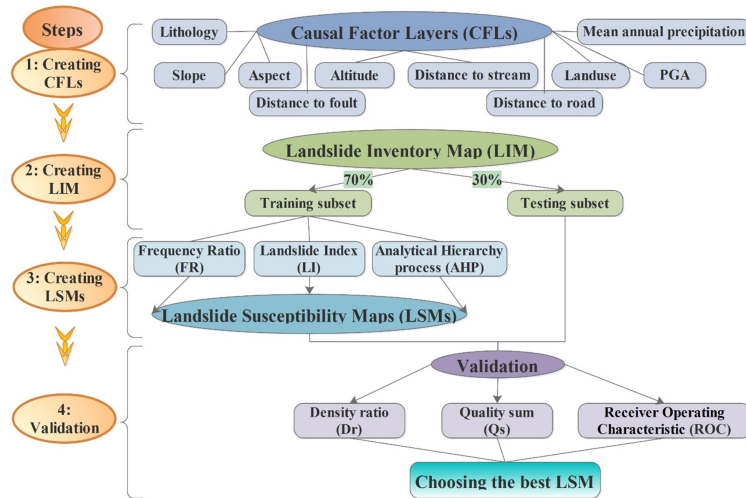**Figure 1.** Location map of Shahroud Watershed in Iran.

Figure 2. Conceptualization flowchart of the study.

including location and area. A preliminary LIM was first produced using the geologic maps, interpretation of aerial photos (1:20,000 scale), historical imagery of Google Earth, and landslide database of the Forests, Rangelands, and Watershed Management Organization of Iran. In the next step, all landslides of preliminary LIM were re-examined during extensive field visits, which lasted about 3 months, and the final LIM was prepared. It should be noted that this research was considered only rotational landslides, therefore the LIM map does not include other types of mass movements such as creep, rock fall, etc. Two examples of landslides investigated in the study area are shown in Figure 3.

<div align="center">(a)   (b)</div>

Figure 3. Two landslides that occurred and their damages: (a) South of Yaroud and (b) South of Viar Villages.

Landslide Causal Factors

Landslide causal factors could be classified into environmental and triggering ones (Wang *et al*., 2014). The triggering group includes external factors that cause immediate changes in the strength/stress of the slopes, resulting in movements such as earthquakes, volcanic eruptions, typhoons, and heavy rainfalls, whereas the environmental group includes potential factors such as slope angle, aspect and lithology (Nguyen and Liu, 2019). The selection of conditioning factors needs to take the characteristics of the study area and data availability into account. In this study, 10 factors including slope, aspect, altitude, land use, lithology, distance to road, distance to stream, distance to fault, Peak Ground Acceleration (PGA), and mean annual precipitation were selected as the main factors that caused landslides of the region (Figure 4). The digital layers of all these factors were prepared in the ArcGIS 10 software environment. The lithological units of the watershed were classified into five classes based on their susceptibility to landslides (Peyrowan and Shariat Jafari, 2013). Factors such as soil depth and dynamics are among other important causal factors that were not included in this analysis due to the lack of relevant data for such a large area as the Shahrood Watershed.

Landslide Susceptibility Mapping

A random systematic method was used to divide LIM dataset into two different subsets: 70% of landslides for training and 30% for testing. The partitioning process was repeated until the ratio of 70 to 30, in addition to the count of landslides, was observed for the area of each subset and landslides of each subset had a suitable spatial distribution on the watershed. In the next step, two statistical models including frequency ratio and statistical index along with the knowledge-based AHP method were used to calculate Landslide Susceptibility Index (LSI).

Frequency Ratio (Fr)

The Fr index is the ratio of landslide occurrence probability to the non-occurrence probability for each class of causal factors (Khan *et al*., 2019). In this method, the first step is calculating the Fr for each category of causal factors (Equation 1). In the next step, the Landslide Susceptibility Index (LSI) was calculated through the summation of Frs (Equation 2).

$$Fr = \frac{L_i / \sum_{i=1}^{n} L_i}{C_i / \sum_{i=1}^{n} C_i} \tag{1}$$

$$LSI = \sum Fr \tag{2}$$

Where, L_i is the area of the landslide in the i-th category for each causal factor, C_i is the area of the i-th category for each causal

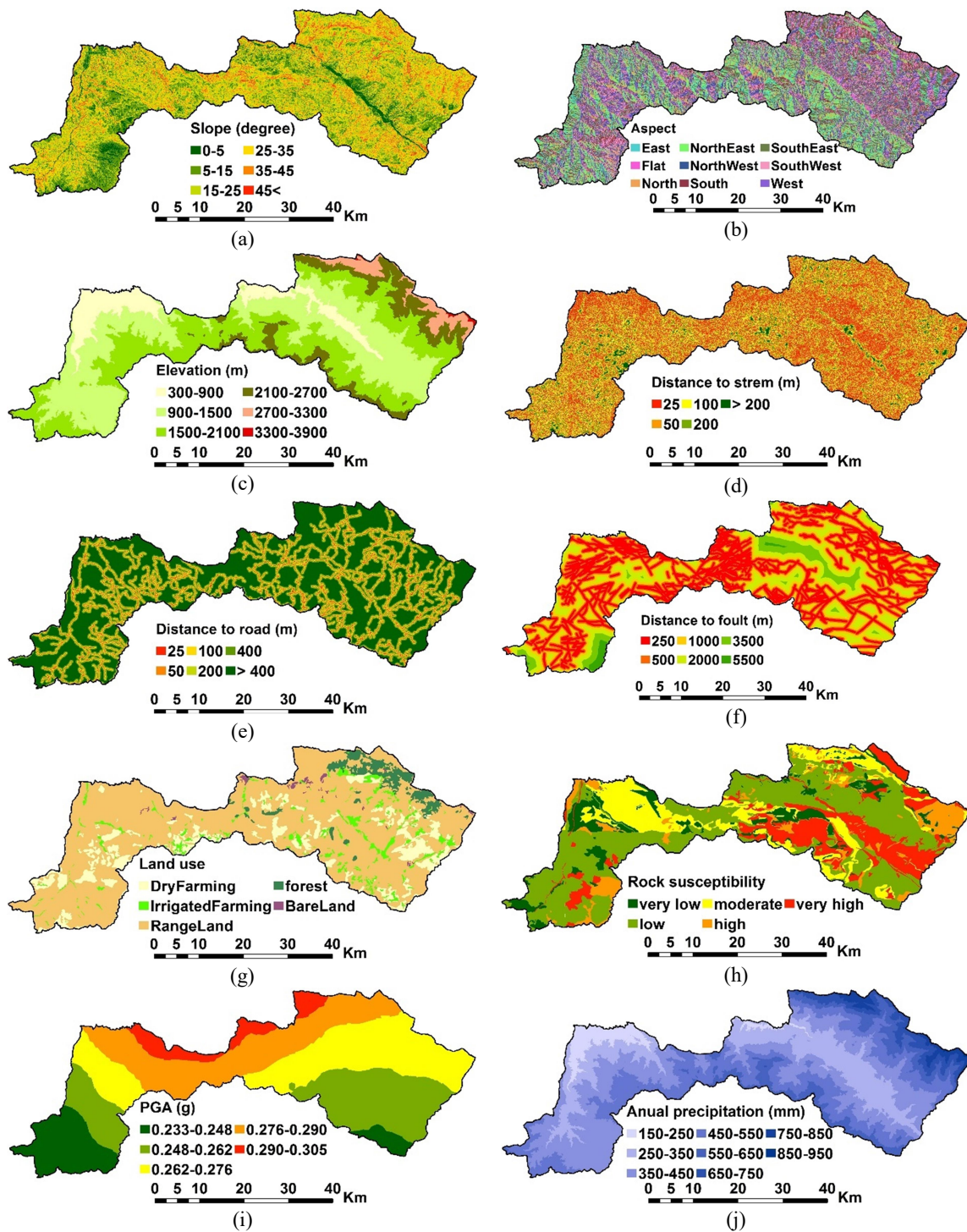<div align="center">698</div>

Figure 4. The maps of landslide causal factors in the study area.

factor, and n is the category number of the causal factor. The interpretation of the resulted values of the Frs is easy and understandable. Fr values greater than 1 indicate a higher probability of landslide occurrence (higher correlation) and values less than 1 indicate a lower probability of landslide occurrence (lower correlation).

Statistical Index (Si)

The statistical index method uses a bivariate statistical approach to calculate landslide susceptibility index (Van Westen, 1997). This method is based on the statistical correlation between the LIM and each class of causal factors. Therefore, the Si values, which is the natural logarithm of the landslide density in the categorical unit divided by the landslide density of the entire map, are calculated for each class of causal factors (Equation 3). Then, the Landslide Susceptibility Index (LSI) is calculated through the summation of Sis (Equation 4).

$$Si = Ln\left(\frac{densclass}{densmap}\right) =$$
$$Ln(\frac{L_i/C_i}{\sum_{i=1}^{n}L_i/\sum_{i=1}^{n}C_i}) \qquad (3)$$

$$LSI = \sum Si \qquad (4)$$

Where, densclass is the landslide density of each class, and densmap is the landslide density within the entire map. In this study, the LIM was crossed separately with every causal factor map to obtain the parameters of this method equation. This method also presents understandable result where positive values of Si imply a higher probability of landslide occurrence and, on the contrary, negative ones indicate a lower probability of landslide occurrence.

AHP Method

The determination of the relative importance levels of the criteria can be achieved by employing Multi-Criteria Decision Analysis (MCDA) methods. The Analytic Hierarchy Process (AHP) is one of the MCDA methods frequently cited in the literature (Turan *et al*., 2020). This method, which was introduced by Saaty (1980), is an easily understood and flexible method to analyze complicated problems such as landslide susceptibility. In this study, a scale from 1-9 was used for pair-wise comparisons and, if the factors had an inverse relationship, a scale of 1/2 -1/9 was used. The Consistency Ratio (CR), which is used to examine the possibility of ranking the factors, was also calculated by Equation (5).

$$CR = \frac{CI}{RI} \qquad (5)$$

Where, CI and RI are, respectively, Consistency Index and Random Consistency index proposed by Saaty (1980). Finally, the various causal factors were integrated based on the weighted linear sum equation (Equation 6) and the Landslide Susceptibility Index (LSI) was produced.

$$LSI = \sum_{i=1}^{n} W_i * X_{ij} \qquad (6)$$

Where W_i is the Weight of ith factor, X_{ij} is the weight of the jth category of ith factor and n is the number of factors. The LSI value ranges in [0, 1] and the greater its value means the higher the LSI.

Validation

To compare the accuracy of the resulting maps, we applied two validation methods by using the 30% testing subset: (1) Receiver Operating Characteristic (ROC) curve and (2) Indices of Density ratio (Dr) and Quality sum (Qs).

In the ROC method, n+1 thresholds are firstly defined for a landslide susceptibility index with n classes (TJPrl, 2006). The first threshold is lower than the minimum LSI and the last one is higher than the maximum LSI. Each threshold made a matrix in which four types of points are defined: True Positive (TP), True Negative (TN), False Positive (FP), and False Negative (FN). TP and FN points are, respectively, the

700

landslides within the classes above and below the threshold value. Conversely, the points of TN and FP are, respectively, stable points within the classes below and the threshold. For each threshold, two statistics called True Positive Rate (TPR) and False Positive Rate (FPR) are calculated based on the numbers of these points as follows:

$$TPR = \frac{TP}{TP+FN} \quad and \quad FPR = \frac{FP}{TN+FP} \quad (7)$$

The ROC curve is drawn by plotting the TPR on the y-axis against the FPR on the X-axis. The Area Under the Curve (AUC) is an indicator to assess the validity of the model such that the higher the area under the curve, the more valid the model is. The AUC values range from 0.5 to 1. An AUC of 0.5 indicates the poor prediction and an AUC of 1 implies perfect prediction.

Based on Dr and Qs indices (Equations 8 and 9), a more valid LSM is a map that creates a better distinction between high-density and low-density landslide areas. Dr indicator is the ratio of landslide density in each susceptibility class to landslide density in the whole study area. A slight deviation of Dr values from the mean value indicates a slight difference in landslide density of different classes and, as a result, the value of the Qs index will be low. According to this, the higher Qs values indicate higher validity of the LSM.

$$Dr = \frac{Si/Ai}{\sum_1^n Si / \sum_1^n Ai} * 100 \quad (8)$$

$$Qs = \sum_{i=1}^n \left[(Dr - 1)^2 \times S \right] \quad (9)$$

Where, Si is the landslide area within the i-th class of LSM, Ai is the area of the i-th class of LSM, S is the ratio of susceptibility class area to the whole area and n is the number of LSM classes.

RESULTS

In Shahroud Watershed, 104 landslides with a total area of 1401 hectares were recorded (Figure 1). The areas of the smallest and largest landslides are 0.1 and 397 hectares, respectively. The mean and the standard deviation of the area of landslides are also equal to 13.4 and 42.5 hectares, respectively. A statistical summary of the landslides used as training and testing subsets is given in Table 1.

Table 2 included the calculated different parameters, which were applied for LSI production of different models. The values of CR calculated in the pairwise comparison matrixes of AHP method range from 0.022 to 0.093 (Appendix I). Considering that all CR values are less than 0.1, the consistency levels are acceptable (Saaty, 1980).

The LSMs of the used models are illustrated in Figure 5. The area of different susceptibility classes for each LSM along with the corresponding landslide area within each class are also presented in Table 3.

The ROC curves of LSMs produced by different models are illustrated in Figure 6. The AUC values of the ROC curve for Fr, Si, and AHP models are equal to 0.707, 0.732, and 0.651, respectively. It is concluded that the LSMs derived from Si and Fr models have good accuracy and the LSM of the AHP model has moderate accuracy in predicting the landslide susceptibility of the Shahroud Watershed.

The chart of density ratio for LSMs derived from used models is presented in Figure 7a. This chart shows an ascending trend of the Dr indicator from low-risk classes to high-risk classes. Therefore, it can be concluded that all three LSMs have been

Table 1. The area (ha) and count of the landslides used as training and testing subsets.

Landslide inventory map		Train (70%)		Test (30%)	
Count	Area	Count	Area	Count	Area
104	1401.3	73	982.8	31	418.5

701

Table 2. The area of causal factor categories, landslides within each category.

Factor	Category	Area (ha)	Landslide area (ha)	Fr	Si	AHP class	weight factor
Slope (Degree)	0-5	11634.3	0	0.0	none	0.029	
	5-15	46727.5	261.08	1.11	0.10	0.046	
	15-25	60250.2	375.26	1.22	0.20	0.076	0.201
	25-35	51946.0	240.80	0.92	-0.08	0.144	
	35-45	19483.2	88.07	0.90	-0.11	0.278	
	45<	4699.7	16.14	0.68	-0.38	0.427	
Aspect	F	1690.6	14.07	1.65	0.50	0.023	
	S	24994.3	219.29	1.74	0.55	0.033	
	SW	25698.1	225.44	1.74	0.55	0.043	
	SE	20274.0	130.81	1.28	0.25	0.060	
	W	20967.9	79.50	0.75	-0.29	0.088	0.029
	E	22801.9	40.75	0.35	-1.04	0.097	
	NW	26919.7	54.15	0.40	-0.92	0.168	
	NE	24433.0	66.59	0.54	-0.62	0.168	
	N	26651.1	150.74	1.12	0.11	0.319	
Altitude (m)	300-900	20750.3	4.58	0.04	-3.13	0.047	
	900-1500	76093.1	286.61	0.75	-0.29	0.074	
	1500-2100	66112.7	552.17	1.65	0.50	0.145	
	2100-2700	22973.1	135.24	1.17	0.15	0.382	0.022
	2700-3300	8260.5	0	0.0	none	0.208	
	3300-3900	530.1	2.75	1.03	0.03	0.144	
Mean annual rainfall (mm)	150-250	9398.5	35.72	0.75	-0.28	0.043	
	250-350	39817.9	410.57	2.04	0.71	0.065	
	350-450	63569.3	382.25	1.19	0.18	0.094	0.107
	450-550	47534.3	126.60	0.53	-0.64	0.156	
	550-650	20976.5	26.20	0.25	-1.40	0.256	
	650-750	9232.6	0	0.0	none	0.386	
PGA (g)	0.233-0.248	24929.4	42.81	0.34	-1.08	0.051	
	0.248-0.262	50862.8	717.11	2.79	1.03	0.078	
	0.262-0.276	57959.1	132.59	0.45	-0.79	0.175	0.072
	0.276-0.290	48292.1	56.14	0.23	-1.47	0.272	
	0.290-0.305	12364.6	32.70	0.52	-0.65	0.424	
Distance to foult (m)	0-250	68529.2	329.81	0.95	-0.05	0.361	
	250-500	41659.4	249.15	1.19	0.17	0.254	
	500-1000	42367.3	317.12	1.48	0.39	0.183	0.047
	1000-2000	29836.5	84.37	0.56	-0.58	0.110	
	2000-3500	10229.7	0.52	0.01	-4.60	0.060	
	3500-5500	1834.3	0.38	0.04	-3.19	0.033	
Distance to stream (m)	0-25	64407.8	392.83	1.21	0.19	0.483	
	25-50	52338.3	293.96	1.11	0.11	0.282	
	50-100	52288.1	222.26	0.84	-0.17	0.111	0.053
	100-200	22166.8	61.47	0.55	-0.60	0.078	
	200<	3255.4	10.83	0.66	-0.42	0.047	

Table 2 continued

Continued of Table 2. The area of causal factor categories, landslides within each category.

| Factor	Category	Area (ha)	Landslide area (ha)	Fr	Si	AHP class	weight factor
Distance to road (m)	0-25	8831.7	34.83	0.781	-0.247	0.379	
	25-50	8229.9	35.62	0.858	-0.153	0.273	
	50-100	14969.3	77.48	1.026	0.025	0.159	0.060
	100-200	25762.9	175.26	1.348	0.299	0.103	
	200-400	40404.2	233.75	1.146	0.137	0.055	
	400<	96258.3	424.40	0.874	-0.135	0.032	
Landuse	Bare land	1280.0	21.47	3.323	1.201	0.035	
	Dry farming	26083.3	149.19	1.133	1/8	0.069	
	Forest	8886.0	72.34	1.613	0.478	0.151	0.131
	Irrigated farming	10390.2	178.51	3.404	1.225	0.248	
	Rangeland	147817.0	559.84	0.750	-0.287	0.497	
Lithology susceptibility	Very low	19600.0	15.67	0.158	-1.842	0.035	
	Low	89082.8	68.01	0.151	-1.889	0.069	
	Moderate	32565.8	161.77	0.984	-0.016	0.151	0.280
	High	18189.6	92.24	1.005	0.005	0.248	
	Very high	35019.7	643.65	3.642	1.293	0.497	

(a)

(b)

(c)
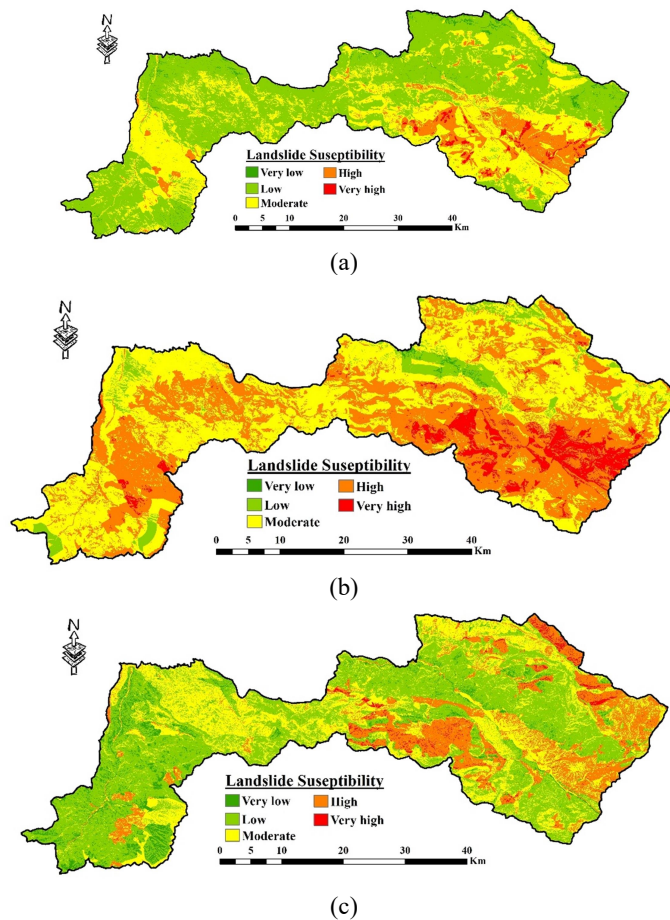
Figure 5. Landslide susceptibility maps developed by models: (a) Frequency ratio (Fr), (b) Statistical index (Si), and (c) Analytical Hierarchy Process (AHP).

703

Table 3. The area (ha) of landslides within each susceptibility class: Ai (area of susceptibility class) and Si (area of landslide within each susceptibility class).

| Model Class	Fr			Si			AHP		
	Ai	Si	Dr	Ai	Si	Dr	Ai	Si	Dr
Very low	3037.3	1.2	0.18	606.8	0.0	0.00	11590.8	0.5	0.02
Low	105664.8	68.2	0.30	11247.7	2.1	0.09	90565.2	79.9	0.41
Moderate	64576.6	167.1	1.20	89264.3	49.3	0.26	56464.7	149.1	1.23
High	19418.2	136.9	3.28	81093.8	230.1	1.32	33314.4	170.9	2.38
Very high	2043.0	45.2	10.30	12527.5	137.4	5.10	2804.8	18.6	3.09
Mean	38948.0	83.7	3.05	38948.0	83.8	1.35	38948.0	83.8	1.43
St.Dev.	45113.5	67.7	4.24	42554.1	98.9	2.16	35558.6	75.9	1.30
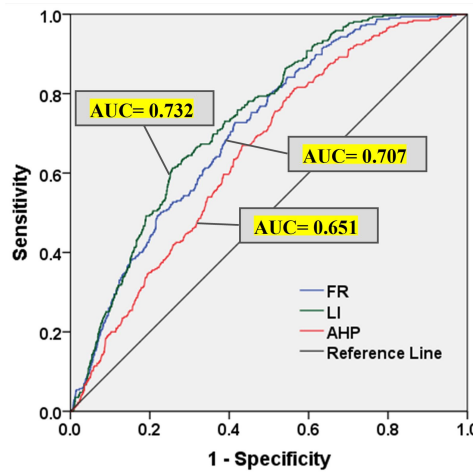
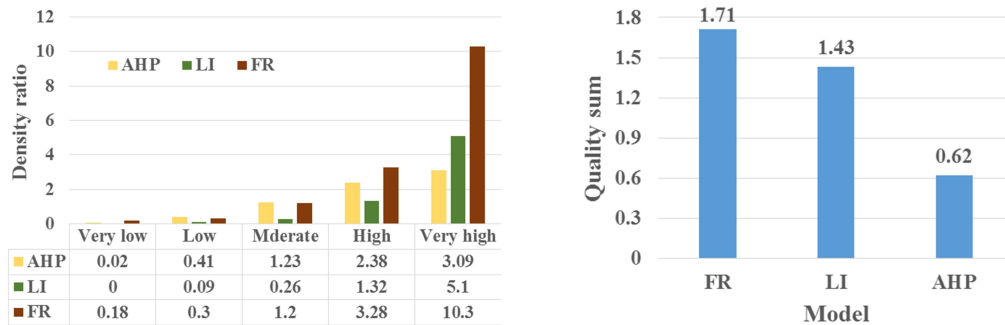**Figure 6.** ROC curves of LSMs produced by different models.

Figure 7. Density ratio (Dr) and Quality sum (Qs) of LSMs derived from different models.

correctly classified. As can be seen in Figure 7b, the value of the Qs index for the AHP model is less than the value of this index for the Fr and Si models, which indicates the lower validity of the LSM derived from the AHP model than the LSMs of the other two models.

DISCUSSION

The results presented in Table 3 imply that in all three models, although the area of the higher susceptible zones is smaller, these

regions usually predict relatively more observed landslides. For example, by Fr model, the very high susceptible class, which covers only 1.05% of the watershed, has predicted about 10.8% of the observed landslides. This makes the Dr indicator have an ascending trend from low susceptible classes to high susceptible classes and implies that all three LSMs have been classified correctly.

This study showed that LSMs obtained from two statistical models are more valid than the LSM derived from the AHP knowledge-based method. In the AHP model, the slight deviation of Dr values from the mean value has caused this model to have a smaller Qs index, which implies less validity of the LSM obtained from the model. The higher validity of the statistical models is confirmed also by the results of ROC curves where more values of AUCs have been calculated for the statistical models. In this regard, previous studies have achieved similar results (Pourghasemi *et al.*, 2012; Sangchini *et al.*, 2016; Yalcin *et al.*, 2011).

The higher accuracy of the used statistical models is due to the fact that these models include the complexity and interaction of various factors affecting the occurrence of landslides (Lee and Pradhan, 2007; Van Westen, 1997). In statistical methods, the weight of classes is calculated based on the previous landslides that have occurred due to the interaction of various causal factors. Based on this, it can be inferred that, in statistical methods, the weights assigned to classes inherently include the interactions of causal factors and the complexities of their occurrence. However, in the pairwise comparisons performed in the AHP method, the preference values of classes are assigned only based on their effect on the occurrence of landslides and without considering the interaction of various causal factors. Therefore, it can be seen in Table 2 that the weights of classes for each causal factor have a regular ascending or descending order, which can be seen similarly in other previous studies (Abay *et al.*, 2019; Achu

and Reghunath, 2017; Pourghasemi *et al.*, 2012; Ruff and Czurda, 2008; Yalcin *et al.*, 2011).

According to Table 2, this ascending or descending order does not exist for the calculated Fr and Si values, except for slope, especially lithology factors. The reason for the exception of lithology and slope factors is the greater contribution of these two factors than other factors in the occurrence of previous landslides. In the Shahroud Mountainous Watershed, the existence of marl formations related to the Miocene and Neogene Periods, which are very susceptible to landslides, is the most important factor in the occurrence of landslides in the region. The greater effect of these two factors can be also seen in the assigned weights of the AHP method, which are equal to 0.280 and 0.201, respectively, for lithology and slope factors. The higher weights of these two factors than other factors have been proven in the results of previous research (Pourghasemi *et al.*, 2012; Salehpour Jam *et al.*, 2021; Yalcin *et al.*, 2011). The dominance of the effect of these two factors has overshadowed the effect of other factors and resulted in the ascending order of Fr and Si values for these two factors. However, the contribution of factors such as aspect, altitude, and distance from linear features such as stream, road, and fault in landslide occurrence has been affected by factors such as lithology, slope, and land use, therefore, no order has been established in their Fr and Si values. The lower weights of factors such as altitude and distance from linear features are in line with the results of previous studies (Pourghasemi *et al.*, 2012; Salehpour Jam *et al.*, 2021; Yalcin *et al.*, 2011).

CONCLUSIONS

This study compared the validity of three conventional models including Fr, Si, and AHP to assess landslide susceptibility in the Shahroud watershed as a hotspot region in landslide occurrence. Since the causes of landslides are many and complex, ten causal

factors including slope, slope aspect, altitude, land use, lithology, distance to road, distance to stream, distance to fault, PGA, and mean annual precipitation were entered into the analyses. However, in this research, some important factors such as soil depth and dynamics were not included in the analysis due to the lack of relevant data for such a large area as the Shahrood watershed. The ascending trend of the Dr indicator from low-risk classes to high-risk classes showed that all three LSMs have been correctly classified. Comparing the validity of the LSMs using the ROC curve and Qs indicator indicated that the two statistical models including Fr and statistical index have presented a more valid LSM than the knowledge-based AHP method. The superior LSM resulting from the most validated model can be a useful tool for planners and policymakers to make better decisions for land use planning and appropriate spatial location of infrastructures. The results of this study can also make a significant contribution to the landslide literature.

ACKNOWLEDGEMENTS

REFERENCES

1. Abay, A., Barbieri, G. and Woldearegay, K. 2019. GIS-Based Landslide Susceptibility Evaluation Using Analytical Hierarchy Process (AHP) Approach: The Case of Tarmaber District, Ethiopia. *Momona Ethiop. J. Sci.,* **11(1)**: 14-36.

2. Achu, A. L. and Reghunath, R. 2017. Application of Analytical Hierarchy Process (AHP) for Landslide Susceptibility Mapping: A Study from Southern Western Ghats, Kerala, India. *Proceedings of the 3rd Disaster, Risk and Vulnerability Conference (DRVC2017),* 29–31 March 2017, Dept. of Geology, Universityof Kerala, India.

3. Armin, M., Mosaffaie, J., Ghorbannia Kheybari, V. and Khairi, A. 2019. Landslide Zoning and Its Risk Management Plan in Kohgiluyeh and Boyerahmad Province Using Haeri-Sami Model. *Quant. Geomorphol. Res.,* **7(4)**: 176-196.

4. Chen, W., Han, H., Huang, B., Huang, Q. and Fu, X. 2017. Variable-Weighted Linear Combination Model for Landslide Susceptibility Mapping: Case Study in the Shennongjia Forestry District, China. *ISPRS Int. J. Geo-Inf.,* **6(11):** 1-16.

5. Chen, W., Zhang, S., Li, R. and Shahabi, H. 2018. Performance Evaluation of the GIS-Based Data Mining Techniques of Best-First Decision Tree, Random Forest, and Naïve Bayes Tree for Landslide Susceptibility Modeling. *Sci. Total Environ.,* **644:** 1006-1018.

6. Dou, J., Yamagishi, H., Pourghasemi, H. R., Yunus, A. P., Song, X., Xu, Y. and Zhu, Z. 2015. An Integrated Artificial Neural Network Model for the Landslide Susceptibility Assessment of Osado Island, Japan. *Nat. Hazards,* **78(3):** 1749-1776.

7. El Jazouli, A., Barakat, A. and Khellouk, R. 2019. GIS-Multicriteria Evaluation Using AHP for Landslide Susceptibility Mapping in Oum Er Rbia High Basin (Morocco). *Geoenvironmental Disasters,* **6(1):** 1-12.

8. Gholami, M., Ghachkanlu, E. N., Khosravi, K. and Pirasteh, S. 2019. Landslide Prediction Capability by Comparison of Frequency Ratio, Fuzzy Gamma and Landslide Index Method. *J. Earth Syst.Sci.,* **128(2):** 1-22.

9. He, H., Hu, D., Sun, Q., Zhu, L. and Liu, Y. 2019. A Landslide Susceptibility Assessment Method Based on GIS Technology and an AHP-Weighted Information Content Method: A Case Study

of Southern Anhui, China. *ISPRS Int. J. Geo-Inf.,* **8(6)**: 1-23.

10. Joybari, J., Kavian, A. A. and Mosaffaie, J. 2017. Effect of Land Use on Landslide Movement in the Tavan District, Qazvin. *Watershed Manag. Res.,* **30(3):** 29-39. (in Persian)

11. Kanungo, D., Arora, M., Sarkar, S. and Gupta, R. 2006. A Comparative Study of Conventional, ANN Black Box, Fuzzy and Combined Neural and Fuzzy Weighting Procedures for Landslide Susceptibility Zonation in Darjeeling Himalayas. *Eng. Geol.,* **85(3-4):** 347-366.

12. Karimi Sangchini, E., Salehpour Jam, A. and Mosaffaie, J. 2022. Flood Risk Management in Khorramabad Watershed Using the DPSIR Framework. *Nat. Hazards,* **114(3):** 3101-3121.

13. Khan, H., Shafique, M., Khan, M. A., Bacha, M. A., Shah, S. U. and Calligaris, C. 2019. Landslide Susceptibility Assessment Using Frequency Ratio, a Case Study of Northern Pakistan. *Egypt. J. Remote Sens. Space Sci.,* **22(1)**: 11-24.

14. Lee, S. 2007. Application and Verification of Fuzzy Algebraic Operators to Landslide Susceptibility Mapping. *Environ. Geol.,* **52(4):** 615-623.

15. Lee, S. and Pradhan, B. 2007. Landslide Hazard Mapping at Selangor, Malaysia Using Frequency Ratio and Logistic Regression Models. *Landslides,* **4(1)**: 33-41.

16. Morady, H. R., Pourghasemi, H. R., Mohammdi, M. and Mahdavifar, M. R. 2010. Landslide Hazard Zoning Using Gamma Fuzzy Operator, with a Case Study of Haraz Watershed. *Environ. Sci.,* **7(4)**: 129-142.

17. Mosaffaie, J. 2016. Application of Artificial Neural Network, Multiple-Regression and Index-Flood Techniques in Regional Flood Frequency Estimation. *Int. J. Water,* **10(4):** 328-342.

18. Mosaffaie, J., Ekhtesasi, M. R., Dastorani, M. T., Azimzadeh, H. R. and Chahuki, M. A. Z. 2015. Temporal and Spatial Variations of the Water Erosion Rate. *Arab. J. Geosci.,* **8(8)**: 5971-5979.

19. Mosaffaie, J. and Salehpour Jam, A. 2018. Economic Assessment of the Investment in Soil and Water Conservation Projects of Watershed Management. *Arab. J. Geosci.,* **11(14):** 1-10.

20. Mosaffaie, J. and Salehpour Jam, A. 2021. Prioritization of Factors Preventing Participation of Rural People in Soil and Water Conservation Projects (The Case of Vers Watershed). *J. Agric. Sci. Technol.,* **23(5):** 975-986.

21. Mosaffaie, J., Salehpour Jam, A. and Sarfaraz, F. 2023. Landslide Risk Assessment Based on Susceptibility and Vulnerability. *Environ. Dev. Sustain.,* **26:** 9285–9303.

22. Mosaffaie, J., Salehpour Jam, A., Sarfaraz, F. and Shadfar, S. 2020. Evaluation of Landslide Susceptibility Zonation applying Fuzzy Gamma Operators in Taleghanroud Watershed of Qazvin Province. *Geogr. Environ. Sustain.,* **36**: 71-90. (in Persian with English Abstract)

23. Nguyen, T. T. N. and Liu, C. -C. 2019. A New Approach Using AHP to Generate Landslide Susceptibility Maps in the Chen-Yu-Lan Watershed, Taiwan. *Sensors,* **19(3)**: 1-18.

24. Oh, H. -J. and Lee, S. 2017. Shallow Landslide Susceptibility Modeling Using the Data Mining Models Artificial Neural Network and Boosted Tree. *Appl. Sci.,* **7(10)**: 1-14.

25. Ozdemir, A. and Altural, T. 2013. A Comparative Study of Frequency Ratio, Weights of Evidence and Logistic Regression Methods for Landslide Susceptibility Mapping: Sultan Mountains, SW Turkey. *J. Asian Earth Sci.,* **64**:180-197.

26. Peyrowan, H. R. and Shariat Jafari, M. 2013. Presentation of a Comprehensive Method for Determining Erodibility Rate of Rock Units with a Review on Iranian Geology. *J. Watershed Eng. Manag.,* **5(3):** 199-213. (in Persian with English Abstract)

27. Pourghasemi, H. R., Moradi, H. R. and Fatemi Aghda, S. M. 2013. Landslide Susceptibility mapping by binary logistic regression, analytical hierarchy process, and statistical Index Models and Assessment of

Their Performances. *Nat. Hazards,* **69(1):** 749-779.

28. Pourghasemi, H. R., Pradhan, B. and Gokceoglu, C. 2012. Application of Fuzzy Logic and Analytical Hierarchy Process (AHP) to Landslide Susceptibility Mapping at Haraz Watershed, Iran. *Nat.Hazards,* **63(2):** 965-996.

29. Pradhan, B., Lee, S. and Buchroithner, M. F. 2009. Use of Geospatial Data and Fuzzy Algebraic Operators to Landslide-Hazard Mapping. *Appl. Geomat.,* **1(1):** 3-15.

30. Pradhan, B., Youssef, A. and Varathrajoo, R. 2010. Approaches for Delineating Landslide Hazard Areas Using Different Training Sites in an Advanced Artificial Neural Network Model. *Geo-Spat. Inf. Sci.,* **13(2):** 93-102.

31. Pradhan, B. and Youssef, A. M. 2010. Manifestation of Remote Sensing Data and GIS on Landslide Hazard Analysis Using Spatial-Based Statistical Models. *Arab. J. Geosci.,* **3(3):** 319-326.

32. Ruff, M. and Czurda, K. 2008. Landslide Susceptibility Analysis with a Heuristic Approach in the Eastern Alps (Vorarlberg, Austria). *Geomorphology,* **94(3-4):** 314-324.

33. Saaty, T. L. 1980. The Analytical Hierarchy Process, Planning, Priority. Resource Allocation. RWS Publications, USA.

34. Salehpour Jam, A., Mosaffaie, J., Sarfaraz, F., Shadfar, S. and Akhtari, R. 2021. GIS-Based Landslide Susceptibility Mapping Using Hybrid MCDM Models. *Nat. Hazards*, **108:** 1025–1046.

35. Salehpour Jam, A., Mosaffaie, J. and Tabatabaei, M. R. 2021a. Assessment of Comprehensiveness of Soil Conservation Measures Using the DPSIR Framework. *Environ. Monit. Assess.,* **193(1):** 1-19.

36. Salehpour Jam, A., Mosaffaie, J. and Tabatabaei, M. R. 2021b. Management Responses for Chehel-Chay Watershed Health Improvement Using the DPSIR Framework. *J. Agric. Sci. Technol.,* **23(4):** 797-811.

37. Salehpour Jam, A., Mosaffaie, J. and Tabatabaei, M. R. 2023. Raster-Based Landslide Susceptibility Mapping Using

Compensatory MADM Methods. *Environ. Model. Softw.,* **159:** 105567.

38. Sangchini, E. K., Emami, S. N., Tahmasebipour, N., Pourghasemi, H. R., Naghibi, S. A., Arami, S. A. and Pradhan, B. 2016. Assessment and Comparison of Combined Bivariate and AHP Models with Logistic Regression for Landslide Susceptibility Mapping in the Chaharmahal-e-Bakhtiari Province, Iran. *Arab. J. Geosci.,* **9(3):** 1-15.

39. Santos, J. G. 2015. GIS-Based Hazard and Risk Maps of the Douro River Basin (North-Eastern Portugal). *Geomat. Nat. Hazards Risk,* **6(2):** 90-114.

40. Saygin, F., Şişman, Y., Dengiz, O. and Şişman, A. 2023. Spatial Assessment of Landslide Susceptibility Mapping Generated by Fuzzy-AHP and Decision Tree Approaches. *Adv. Space Res.*, **71(12):** 5218-5235.

41. Soltani, M. J., Motamedvaziri, B., Mosaffaei, J., Noroozi, A. A. and Ahmadi, H. 2023. Cause and Effect Analysis of the Trend of Dust Storms Using the DPSIR Framework in the Hendijan Region. *Int. J. Environ. Sci. Technol.*, **20:** 4919–4930.

42. TJPrl, F. 2006. An Introduction to ROC Analysis. *Pattern Recogn. Lett.,* **27(8):** 861-874.

43. Turan, İ. D., Özkan, B., Türkeş, M. and Dengiz, O. 2020. Landslide Susceptibility Mapping for the Black Sea Region with Spatial Fuzzy Multi-Criteria Decision Analysis under Semi-Humid and Humid Terrestrial Ecosystems. *Theor. Appl. Climatol.,* **140(3):** 1233-1246.

44. Van Westen, C. 1997. Statistical Landslide Hazard Analysis. *Ilwis,* **2:** 73-84.

45. Wang, M., Liu, M., Yang, S. and Shi, P. 2014. Incorporating Triggering and Environmental Factors in the Analysis of Earthquake-Induced Landslide Hazards. *Int. J. Disaster Risk Sci.,* **5(2):** 125-135.

46. Yalcin, A., Reis, S., Aydinoglu, A. C. and Yomralioglu, T. 2011. A GIS-Based Comparative Study of Frequency Ratio, Analytical Hierarchy Process, Bivariate Statistics and Logistics Regression Methods for Landslide Susceptibility Mapping in

مقایسه کارایی روش‌های آماری و دانش محور پهنه بندی حساسیت زمین لغزش

ج. مصفایی، ا. صالح پورجم، و م. ر. طباطبائی

چکیده

وقوع مکرر زمین‌لغزش در آبخیز شاهرود خسارات جانی و مالی فراوانی را به بار آورده است. لذا، پهنه‌بندی حساسیت زمین‌لغزش برای کاهش خسارات ناشی از آن ضروری است. هدف از این تحقیق، مقایسه نقشه‌های حساسیت زمین‌لغزش حاصل از روش‌های مختلف است. ابتدا لایه‌های موضوعی ده عامل موثر بر زمین‌لغزش تهیه شد. سپس نقشه پراکنش زمین‌لغزش شامل ۱۰۴ زمین‌لغزش به مساحت ۱۴۰۱ هکتار تهیه و به دو زیرمجموعه شامل ۷۰ درصد برای آموزش مدل‌ها و ۳۰ درصد برای آزمایش مدل‌ها تقسیم شد. سه نقشه حساسیت زمین‌لغزش با استفاده از روش‌های نسبت فراوانی، شاخص آماری و تحلیل سلسله‌مراتبی تهیه شد. فرآیند اعتبارسنجی مدل‌ها نشان داد که مدل‌های شاخص آماری (AUC = 0.732) و نسبت فراوانی (AUC = 0.707) نقشه‌های معتبرتری را نسبت به روش AHP (AUC = 0.651) ارائه کرده‌اند. همچنین مقادیر شاخص Qs، نتایج اعتبارسنجی حاصل از منحنی ROC را تایید می‌کند. براین اساس، مقادیر شاخص Qs به ترتیب برابر با ۱.۷۱، ۱.۴۳ و ۰.۶۲ برای مدل‌های نسبت فراوانی، شاخص آماری، و AHP است که دلالت بر نقشه‌های پهنه‌بندی دقیق‌تر مدل‌های نسبت فراوانی و شاخص آماری نسبت به نقشه حاصل از روش AHP دارد. نتایج این مطالعه می‌تواند برای مدیریت خطر زمین‌لغزش در منطقه مورد استفاده قرار گیرد.